

Deposition of Ti_xC layers on TiC hardmetals

K. BARTSCH, A. LEONHARDT, E. WOLF, M. SCHÖNHERR, M. SEIDLER
*Central Institute of Solid State Physics and Material Science, Academy of Science of the GDR,
 8027 Dresden, Helmholtzstrasse 20, GDR*

The chemical vapour deposition of Ti_xC layers on nickel-containing hardmetals is often connected with the formation of small inclusions within the layers depending on the stoichiometry x . The inclusions were identified as the Ni_3Ti intermetallic compound, which is formed if x exceeds 1.03. It was found that the deposition of high stoichiometric and, consequently, inclusion-free Ti_xC layers is difficult in the kinetically controlled region of the hydrocarbon decomposition used as carbon carrier in the gas phase (for example C_6H_6 , CH_4). It was shown by special experiments, that the intermetallic phase is formed by chemical reaction between the gas phase and solid nickel, which comes into contact with the gaseous components by surface and grain-boundary diffusion processes through the layer. It is possible to reduce or to avoid the formation of inclusions by the substitution of nickel by cobalt or iron as binding metals due to the decreasing thermodynamic stability of the metal-rich intermetallic phases.

1. Introduction

In recent years the interest in WC-free hardmetals (e.g. TiC-Mo₂C-Ni and TiCN-Mo₂C-Ni hardmetals) has grown. Their performance as cutting tools has particularly been investigated and compared with that of WC-Co hardmetals [1]. In some cases the cutting properties of both types of hardmetals are similar. Contrary to WC-Co hardmetals, the deposition of hard coatings, e.g. Ti_xC , TiC_xN_y , TiN, Al_2O_3 , on nickel-containing hardmetals by CVD has never resulted in an important enhancement of wear resistance, hitherto. A drastic lowering of cutting properties was observed in many cases, apparently due to precipitations of intermetallic compounds formed by chemical interactions with the nickel binder during the CVD process.

It is the purpose of this work to determine the reasons for the formation of intermetallic phases during the deposition of TiC layers on nickel-containing hardmetals. Furthermore, the variation of reactivity of the binder metal when substituting nickel by cobalt or iron has been investigated.

2. Experimental procedure

Hardmetals on the basis of TiC and Mo₂C or TiCN and Mo₂C, with a nickel-binder content between 10 and 20 wt %, have been coated with TiC layers by CVD. WC-Co hardmetals, cobalt- and iron-bound hardmetals, as well as inert substrates, have also been applied in some cases.

Very often kinetic effects are dominant in CVD processes. For example, the reactor type (hot wall or cold wall) and the reactivity of the carbon-delivering compound influence the layer formation. Therefore experiments were performed both under near-equilibrium conditions and under kinetic control.

As starting substances, in addition to hydrogen and

$TiCl_4$, the rather inert benzene or the more reactive heptane have been used. The deposition process was realized in a tube reactor heated by an electric furnace (HWR), and in a cold wall reactor (CWR) with inductive substrate heating. In both cases the samples were horizontally arranged, so that the flow conditions were similar. Because conditions for the thermal activation of the reaction gases are more favourable in the HWR, the equilibrium state is attained in the HWR rather than in the CWR. The applied deposition parameters are summarized in Tables I and II (p^{x_0} = balance pressure in the initial state).

In order to characterize the deposited layers the samples were investigated by metallographic techniques, X-ray diffraction, EPMA and chemical analysis.

3. Results

3.1. Deposition with benzene

Figs 1a and b exhibit a layer structure, which is typical for nickel-containing hardmetals (deposition according to no. 1, Table I), and for the purpose of comparison the cross-section of a WC-Co hardmetal coated under the same conditions. Contrary to the single-phase TiC layer on the WC-Co hardmetal, the layer on the nickel-containing substrate contains numerous inclusions within the whole layer. Furthermore, pores and an enrichment of a bright phase at the phase boundary are visible in this sample. The inclusions could be identified as $TiNi_3$ by X-ray diffraction measurements, and according to EPMA investigations an enhanced nickel content is detected at the phase boundary. The formation of nickel-containing precipitations could be avoided at $T = 1293$ K only by a high benzene concentration in the gas phase (no. 2, Table I). However, the layers deposited in CWR always revealed precipitations (nos 8 and 9, Table I). From Table I the influence of deposition temperature

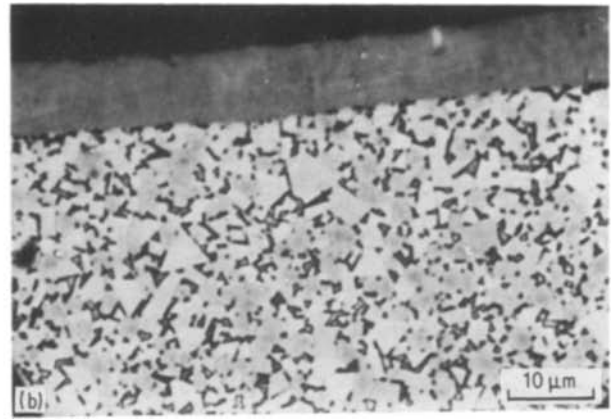
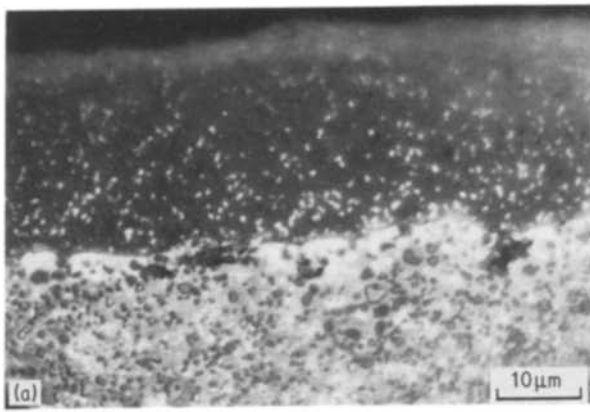


Figure 1 Ti_xC layers on hardmetals. (a) TiC–Mo₂C–Ni hardmetal. (b) WC–Co hardmetal.

also follows. At the highest and lowest deposition temperatures, no precipitation or only single precipitations occurred, respectively. Because the deposition rate strongly approaches zero, a further decrease of the deposition temperature below $T \approx 1223$ K was not practicable.

In the case of the cobalt-bound TiC hardmetals (binder content ~ 13 wt %) layers deposited according to no. 1, were free of precipitations, whilst samples coated according to no. 8 contained relatively strong precipitations (Fig. 2). If iron was the main binder component (e.g. 13% Fe, 2% Ni, 5% Co), layers according to no. 8 were deposited, also without precipitations.

3.2. Deposition with heptane

The deposition of precipitation-free TiC layers on nickel-bound hardmetals in the HWR is realized with heptane rather than with benzene. The results of metallographic layer examination are given in Table II. Some layer compositions determined by chemical analysis are also given in Table II. The analytical samples were obtained by deposition on inert substrates and subsequent mechanical isolation. Examples for the beginning of the formation of TiNi₃ are shown in Fig. 3.

TiC hardmetals with cobalt or iron binder (binder content 20 wt %) coated according to no. 10 did not form precipitations.

In the CWR, nickel-containing substrates could be coated precipitation-free only according to no. 21.

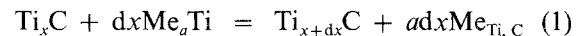
Proceeding from no. 17 to no. 20, a reduction of the number of precipitations was observed with growing p_C^{xo}/p_{Ti}^{xo} ratio. Comparing the deposition rate of TiC on TiC–Ni hardmetals to that of WC–Co hardmetals, it can be stated that the deposition rate of the precipitation-containing layers is higher (see Fig. 4). With a decreasing number of precipitations, the curves of TiC–Mo₂C–Ni and WC–Co substrates, approach each other.

4. Discussion

4.1. Thermodynamics

Figs 5a to c show the ternary phase diagrams of the systems Me–Ti–C (Me = Fe, Co, Ni) at 1300 K [2]. The stoichiometry x in Ti_xC – this notation was chosen for practical reasons, at the coexistence point of three solid phases is fixed by the temperature, and in the coexistence range of two solid phases by the temperature and composition of the coexisting solid phase. Therefore a critical stoichiometry of Ti_xC has to be realized in deposition of Ti_xC on TiC hardmetals, if interactions with the substrate are to be avoided.

There are no data for the composition of Ti_xC at the coexistence points with the other phases. But it is possible to calculate these compositions from the thermodynamic data of the coexisting phases. Starting from the non-equilibrium reaction



and the coexistence condition $d\Delta G_R^0(1)/dx = 0$ one

TABLE I Deposition of Ti_xC layers with benzene

No.	Type of reactor	Deposition conditions			Growth rate* ($\mu\text{m h}^{-1}$)	Precipitations*
		$\frac{p_C^{xo}}{p_{Ti}^{xo}}$	$\frac{P_H^{xo}}{p_{Ti}^{xo} + p_C^{xo}}$	T (K)		
1	HWR	3	18	1293	12	numerous
2		4	4.5	1293	16	none
3	HWR	3	10	1223	20	isolated
4		3	10	1273	30	numerous
5		3	10	1323	37	numerous
6		3	10	1373	74	numerous
7		3	10	1403	310	none
8	CWR	3	18	1293	42	numerous
9		4	4.5	1293	73	numerous

*Valid for layers on nickel-containing substrates.

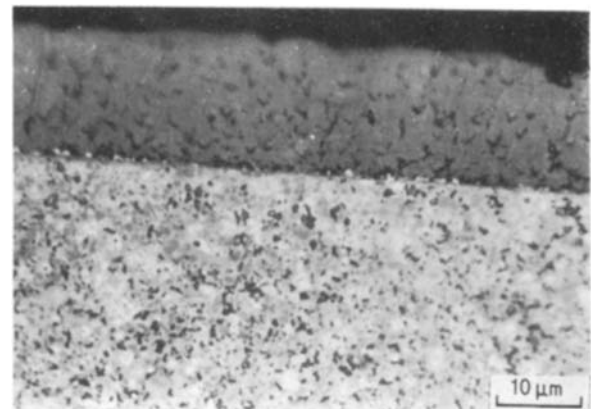


Figure 2 Ti_xC layer on TiC–Mo₂C–Co hardmetal.

TABLE II Deposition of Ti_xC layers with heptane: $T = 1293\text{ K}$, $p_H^{xO}/(p_{Ti}^{xO} + p_C^{xO}) = 20$

No.	Type of reactor	Deposition conditions, p_C^{xO}/p_{Ti}^{xO}	Precipitations*	x in Ti_xC^\dagger
10	HWR	0.1	numerous	-
11		0.2	numerous	1.19
12		0.3	some	1.09
13		0.35	isolated	1.04
14		0.4	none	1.02
15		0.5	none	-
16		0.7	none	-
17	CWR	1.0	numerous	
18		1.5	numerous	
19		2.0	numerous	
20		3.0	numerous	
21		4.0	isolated	

*Valid for layers on nickel-containing substrates.

†Valid for layers on inert substrates.

obtains:

$$\frac{d\Delta G_f^0(Ti_xC)}{dx} = \Delta G_f^0(Me_aTi) - a [\bar{G}(Me_{Ti,C}) - G^0(Me)]$$

where Me_aTi is the Me-richest intermetallic compound at the upper phase boundary, $Me_{Ti,C}$ is the metal, saturated with titanium and carbon, $\Delta G_R^0(1)$ is the standard free energy of Reaction 1, ΔG_f^0 is the standard free energy of formation from the elements, \bar{G} is the partial free energy, and G^0 is the standard free energy.

Analogous relations can be applied to the coexistence of two intermetallic compounds with Ti_xC and to the coexistence of Ti_xC with the solid solution of carbon and titanium in the metal. Calculations were done for all possible cases of coexistence of Ti_xC with Me_aTi in the systems Me-Ti-C. The results, as well as the data used, are given in Table III. Because the solubility of carbon and titanium in Me is small, the free energies of Me were taken for the free partial molar energies, i.e. the term in the angular brackets of Relation 1 was set equal to zero.

4.2. Explanation of the experimental observations

From the results of the thermodynamic calculations it

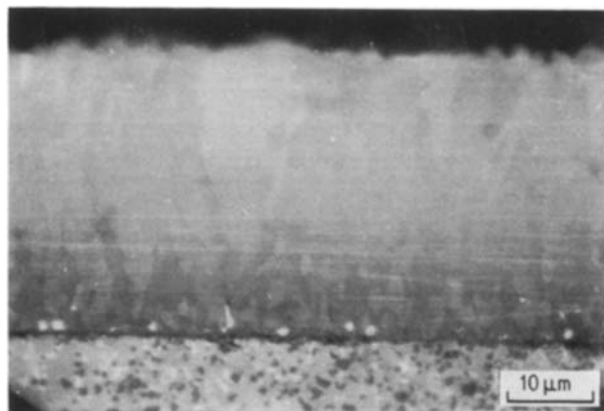


Figure 3 First precipitations of $TiNi_3$ in a Ti_xC layer deposited with heptane.

TABLE III Coexistence compositions of Ti_xC in the systems Me-Ti-C (Me = Ni, Co, Fe) and thermodynamic data of the coexisting phases, $T = 1300\text{ K}$; $d\Delta G_f^0 Ti_xC/dx = -593.366 + 550.129x - 126.014x^2$

Coexisting phases	$-\Delta G_f^0$ (kJ mol ⁻¹)	Reference	x in Ti_xC
$Ni_{Ti,C}$	0		
$TiNi_3$	160.31	[3]	1.03
$TiNi_3$	160.31	[3]	
$TiNi$	75.15	estimated	1.62
$Co_{Ti,C}$	0		
Co_3Ti	121.46	estimated	1.17
Co_3Ti	121.46		
Co_2Ti	96.38	estimated	1.53
Co_2Ti	96.38		
$CoTi$	61.71	estimated	1.66
$Fe_{Ti,C}$	0		
Fe_2Ti	64.56	[4]	1.43
Fe_2Ti	64.56		
$FeTi$	47.94	[4]	1.63

can be expected that the formation of $TiNi_3$ would take place at small deviations of the composition of Ti_xC from the composition limit of pure Ti_xC ($x = 1$). In the deposition of Ti_xC layers with benzene, the stoichiometry of Ti_xC does not reach the value expected by thermodynamic calculations [5], regardless of the type of reactor used (HWR or CWR). Therefore the formation of $TiNi_3$ is not surprising in this case. For example, x amounts approximately to 1.25 in Ti_xC , which was deposited according to no. 1 (Table I) on silica substrates and analysed by chemical analysis. The $TiNi_3$ formation may be avoided by an extreme benzene content in the gas phase (no. 2); however, it is uncertain if the equilibrium composition according to the phase diagram is deposited. Analogous samples deposited under the same conditions on silica and investigated by chemical analysis contained free carbon to a considerable amount, though part of the bound carbon was comparable to that of samples produced according to no. 1.

It is possible to overcome the kinetic restraints partially by increasing the deposition temperature. As established by chemical analysis, the content of bound carbon grows with deposition temperature, and precipitation-free layers can also be obtained with benzene (Table I, no. 7). As expected, the kinetic

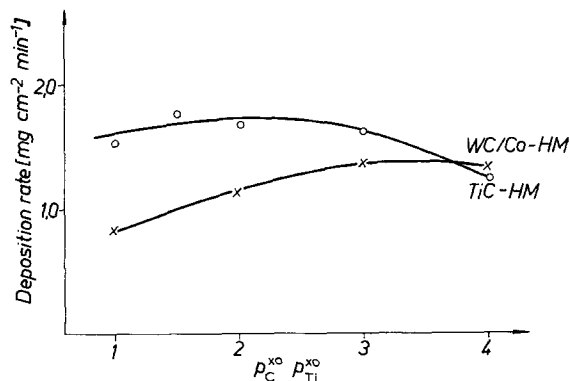


Figure 4 Deposition rate of Ti_xC layers on WC-Co and TiC-Mo₂C-Ni hardmetals.

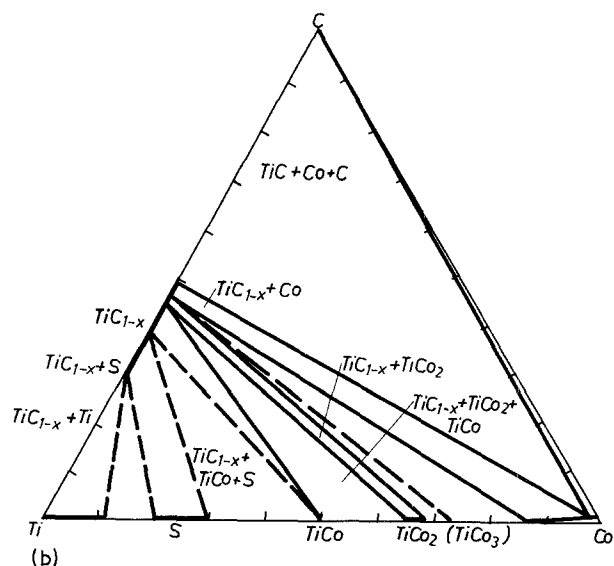
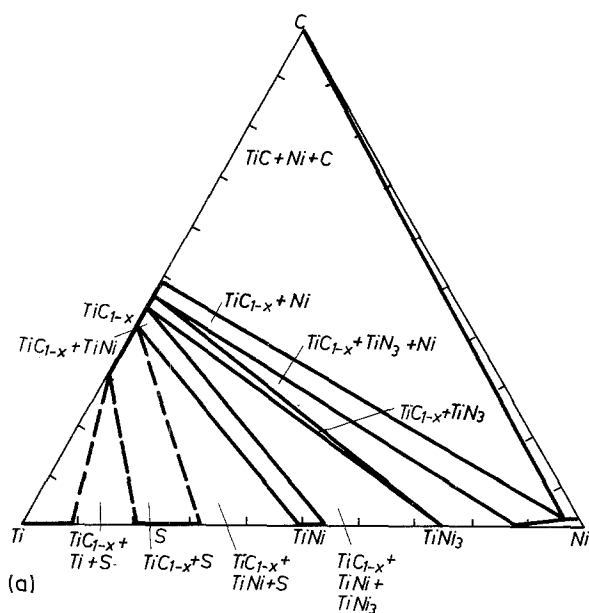
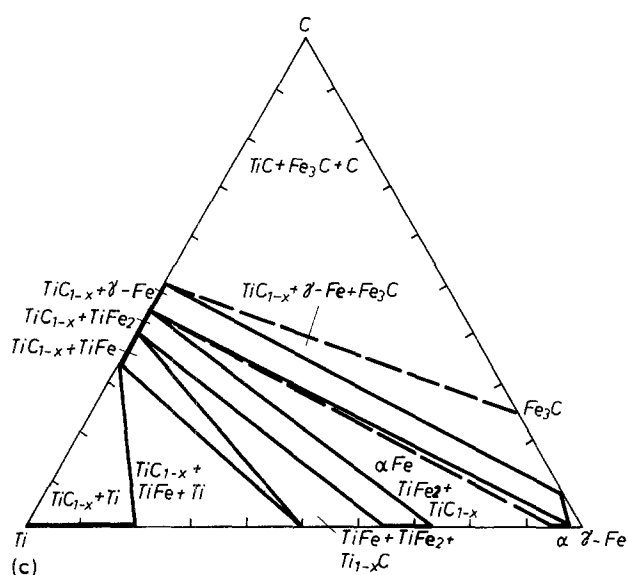


Figure 5 Phase diagrams of the systems Me-Ti-C. (a) Ni-Ti-C. (b) Co-Ti-C. (c) Fe-Ti-C.



effects are more effective in the CWR than in HWR (Table I, no. 9).

Using heptane as the carbon-delivering compound in the deposition process, the composition of Ti_xC approaches the equilibrium composition in HWR. In Table II stoichiometries of Ti_xC are given, which are in a rather good agreement with thermodynamic calculations of the system Ti-C-Cl-H [5].

The experimentally determined value $x = 1.04$ for the starting formation of $TiNi_3$ supports the calculated value $x = 1.03$. Unlike the HWR, in CWR the equilibrium state is not reached in most cases. Only at a heptane content in the deposition gas far away from the theoretical value can the formation of precipitations be avoided (Table II, no. 21).

As shown in Section 4.1, the tendency to form intermetallic precipitations should decrease in the sequence Ni-Co-Fe. Preliminary investigations with cobalt- and iron-bound TiC-hardmetals confirmed this assumption. Thus the cobalt-containing substrates could be precipitationless coated in HWR (nos 1, 10) and the mainly iron-containing substrates in HWR (nos 1, 10) and CWR (no. 8).

In the same way intermetallic precipitations have

never been observed in TiC layers deposited on WC-Co hardmetals, because the formation of η -carbides takes place in the substrate and the layers are partially carburized when depositing a Ti_xC of low stoichiometry.

In principle the metallographic micrographs of precipitation-containing layers were always similar to Fig. 1a. It is evident that no typical reaction zone is formed, as observed, for example, in diffusion-controlled solid-solid reactions [7, 8]. The distribution of the $TiNi_3$ inclusions in the layer, as well as some other observations, point to a possible influence of the gas phase in the formation of the precipitations. Thus it is assumed that the increased deposition rates on nickel-containing substrates (Fig. 4) are due to an additional incorporation of titanium from the gas phase during $TiNi_3$ formation.

Fig. 6 shows a layer sequence, which consists of a TiCN layer formed by Plasma CVD at low temperatures ($T = 1123$ K) and a subsequent normal CVD Ti_xC layer deposited with benzene at 1293 K. The TiCN layer and the initial range of the Ti_xC layer are free from precipitations. Probably the nickel diffusion during the plasma-CVD process is negligible. In the subsequent Ti_xC deposition at 1293 K a precipitation-free layer grows at the beginning of the process, i.e. during that time which the nickel of the substrate needs for penetration of the relatively thick TiCN layer. The formation of $TiNi_3$ begins when nickel reaches the phase-boundary solid-gas.

We also observed that layers containing precipitations show no preferred orientation, as in the case of Ti_xC deposition on WC-Co substrates [9]. Because of the simultaneous formation of $TiNi_3$ precipitations by gas-solid reactions, the growth of fibre crystals and their orientation in the growth direction of the layer is disturbed. After annealing of samples with $TiNi_3$ inclusions at 1293 K, no alteration in the layers was observed by metallographic examination. Obviously solid-solid interactions do not contribute to a larger

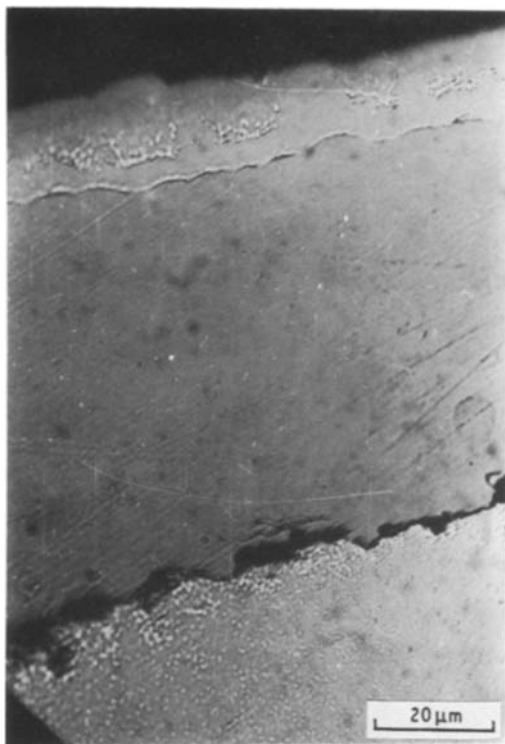


Figure 6 Ti_xC layer (C_6H_6) on an intermediate TiCN layer (TiCN deposited by PACVD).

extent to the formation of $TiNi_3$. A diffusion coefficient for nickel of the magnitude 10^{-8} to 10^{-9} cm^2 sec^{-1} can be estimated for both benzene Ti_xC and heptane Ti_xC layers from experimental observations. The high velocity of the nickel transport to the solid-gas phase boundary points to surface and grain-boundary diffusion. The nickel content of both types of layer determined by EPMA was about 1 wt % in precipitation-free regions of the layers.

Finally it is noteworthy, that the discussed phenomena were observed in a similar manner for $TiC-Mo_2C$ and $TiCN-Mo_2C$ hardmetals. Therefore, distinction between the substrates was not necessary in the discussion of the experimental results. Similar effects to those observed in the deposition of Ti_xC were also established in deposition of TiCN and TiN layers.

5. Conclusions

In the deposition of Ti_xC layers on $TiC-Mo_2C$ and

$TiCN-Mo_2C$ hardmetals, by CVD $TiNi_3$ inclusions takes place at low deviations of the Ti_xC stoichiometry from the carbon-rich limiting composition. Using hydrocarbons with low reactivity (for example, benzene, methane) as carbon-delivering compounds, the deposition of precipitation-less high stoichiometric Ti_xC layers is strongly limited. The formation of precipitations takes place by interaction of the deposition gas phase with nickel diffusing from the substrate into the layer. The transport of nickel through the layer proceeds via diffusion along grain boundaries and inner surfaces.

In the sequence of the binder metals Ni-Co-Fe the tendency to form intermetallic compounds decreases, so that the undesired formation of intermetallic compounds can be decreased by substitution of nickel with cobalt and iron.

Acknowledgements

We thank Dr. Klosowski for the EPMA, Dr. Henke for the X-ray-analysis and Dr Friedrich for the chemical analysis.

References

1. K. MÜLLER, A. BEGER, W. FÖRSTER, G. GILLE, H. KOTSCH, G. PUTZKY and D. SELBMANN, Proceedings, VIII International Pulvermetall. Tagung, Dresden, 24 to 26 September (1985) Bd. 3, S. 32.
2. H. HOLLECK and H. KLEYKAMP, *Int. J. Refractory Hardmetals* **1** (1982) 112.
3. G. CHATTOPADHYAY and H. KLEYKAMP, *Z. Metallkde* **74** (1983) 182.
4. J. BARIN, O. KNACKE and O. KUBASCHEWSKI, "Thermochemical properties of inorganic substances", Supplement, (Springer Verlag, Düsseldorf, 1977).
5. D. SELBMANN, E. WOLF and M. SCHÖNHERR, Proceedings 3rd Fachtagung "Nichtmetallisch-anorganische Schutzschichten" (TH Karl-Marx-Stadt, 1981) S. 32-38.
6. A. LEONHARDT, M. SEIDLER, K. BARTSCH, D. SELBMANN, M. SCHÖNHERR and E. WOLF, *J. Less-Common Metals* **87** (1982) 71.
7. P. P. J. RAMAEKERS, F. J. J. van LOO and G. F. BASTIN, *Z. Metallkde* **76** (1985) 245.
8. *Idem, ibid.* **75** (1984) 639.
9. A. LEONHARDT, D. SCHLÄFER, M. SEIDLER, D. SELBMANN and M. SCHÖNHERR, *J. Less-Common Metals* **87** (1982) 63.

Received 23 October 1986

and accepted 22 January 1987